HHS Public Access

Author manuscript

*Ophthalmol Retina*. Author manuscript; available in PMC 2020 April 01.

Published in final edited form as:

*Ophthalmol Retina*. 2019 April ; 3(4): 316–325. doi:10.1016/j.oret.2018.11.011.

# Distribution of OCT features within areas of macular atrophy or scar after two years of anti-VEGF treatment for neovascular AMD in CATT

**Cynthia A. Toth**[1,4], **Vincent Tai**[1], **Maxwell Pistilli**[2], **Stephanie J. Chiu**[1], **Katrina Winter**[1], **Ebenezer Daniel**[2], **Juan E. Grunwald**[2], **Glenn J. Jaffe**[1], **Daniel F. Martin**[3], **Gui-shuang Ying**[2], **Sina Farsiu**[4], and **Maureen G. Maguire**[2] **Comparison of Age-related Macular Degeneration Treatments Trials (CATT) Research Group**

[1]Department of Ophthalmology, Duke University, Durham, North Carolina

[2]Department of Ophthalmology, University of Pennsylvania, Philadelphia, PA

[3]Cole Eye Institute, Cleveland Clinic, Cleveland, OH

[4]Department of Biomedical Engineering, Duke University, Durham, NC

## Abstract

**Purpose:** Macular atrophy and scar increase in prevalence during treatment for neovascular age-related macular degeneration (AMD) and are associated with poor visual acuity. We sought to identify the distribution of spectral domain optical coherence tomography (SDOCT)-determined features and subretinal lesion thicknesses at sites of macular scar or atrophy after two years of treatment in the Comparison of AMD Treatments Trials (CATT).

**Design:** Cross-sectional analysis

**Participants:** CATT participants with SDOCT, color photograph and fluorescein angiogram (CP/FA) images at Year 2.



ClinicalTrials.gov number NCT00593450.

Disclosures:
Cynthia A. Toth, Alcon Laboratories, unrelated royalties, unlicensed patents on OCT analyses
Vincent Tai: none
Maxwell Pistilli; none
Stephanie J. Chiu, unlicensed patents on OCT analyses
Katrina Winter; none
Ebenezer Daniel; none
Juan E. Grunwald; none
Glenn J. Jaffe; Heidelberg Engineering (Consultant), Novartis (Consultant), Regeneron (Consultant).
Daniel F. Martin; none
Gui-shuang Ying, Chengdu Kanghong Biotech co. Ltd :Code C (Biostatistical Consultant);Ziemer Ophthalmic Systems AG (Biostatistical consultant).
Sina Farsiu; unlicensed patents on OCT analyses
Maureen G. Maguire, Genentech/Roche (Data and Safety Monitoring Committee)

**Methods:** Sixty-eight study eyes at Year 2 in CATT, were selected based on image quality and CP/FA-determined predominant presence of: geographic atrophy (GA, n=25), non-GA (NGA, n=44), fibrotic scar (FS, n=26) or non-FS (NFS, n=7). CP/FA components were delineated by CP/FA readers; SDOCT morphologic features and thicknesses were delineated by OCT readers. Using custom software and graphic user interfaces, images were registered, overlaying features and components per pixel; differences were analyzed across groups.

**Main Outcome Measures:** OCT features, CP/FA components, and retinal and subretinal lesion thicknesses at each pixel of regional overlays.

**Results:** SDOCT assessment of registered areas of pathology revealed the following: 1) retinal pigment epithelium atrophy (with or without residual lesion material) covered 75% of pixels designated as GA, 22% as NGA, 24% of NFS and 46% of FS ($p<0.001$); 2) photoreceptor layer thinning covered 85% of GA, 42% of NGA, 33% of NFS and 59% of FS ($p<0.001$); 3) subretinal lesion features covered 31% of GA, 42% of NGA, 85% of NFS, and 92% of FS ($p<0.001$). Mean thickness of the subretinal lesion complex (microns ± standard deviation) differed between GA (48±25), NGA (61±35), NFS (83±17), and FS (151±74) ($p<0.001$). In eyes with GA the thickness was greater in areas with residual lesion (51.4±27) than in those without (27.2±9).

**Conclusions:** RPE atrophy and photoreceptor layer thinning are common not only in areas of macular atrophy but in areas of fibrotic scar. Photoreceptor loss extends beyond the areas of clinically apparent atrophy and fibrotic scar. Subretinal lesion components were common in areas of scar, but were also present in nearly 1/3 or more of areas of macular atrophy.

## Precis:

After two years of anti-VEGF therapy for neovascular age-related macular degeneration, optical coherence tomography imaging reveals a range of retinal features and subretinal lesion thicknesses at sites of macular scar or atrophy.

## Introduction:

Despite early recovery of visual acuity with anti-VEGF treatment in the majority of eyes with active subfoveal neovascular age-related macular degeneration (nAMD), visual acuity in these eyes typically declines over subsequent years of treatment. We lack a clear understanding of the complex inter-related microanatomic changes in nAMD, their evolution during antiVEGF treatment and their relationship to concurrent and future visual acuity. These relationships have been studied in nAMD through analysis of retinal images, most commonly, color photographs (CP), fluorescein angiograms (FA) and optical coherence tomography (OCT). Many of the analyses correlating the findings across imaging modalities have centered on the presence and location of fluid surrounding the neovascularization, and in particular on areas of fluid leakage designated as intraretinal fluid (IRF), subretinal fluid (SRF) and sub-retinal pigment epithelial (sub-RPE) fluid on OCT imaging.

Both geographic atrophy and scar are more prevalent at two years after the start of anti-VEGF treatment than at baseline[1–5], and the presence of each of these pathological feature is associated with poorer visual acuity[6, 7]. However, on CP and FA it is not possible to distinguish the retinal and subretinal components of these late-stage lesions.

There is a robust body of evidence to demonstrate the relationship between fluid location on OCT images in nAMD and visual acuity before and after anti-VEGF treatment,[6, 8, 9] and to link atrophy and scar to visual acuity loss during antiVEGF treatment.[4, 7, 10–12] However, analyses that assess the relation of OCT features to specific regions of macular atrophy, geographic atrophy or scar based on CP/FA after anti-VEGF treatment are lacking. We hypothesized that if we could accurately and precisely correlate information from CP/FA and OCT, at a specific pathology site, that we would identify common retinal and subretinal anatomic elements that would help to explain visual acuity loss, thus identifying a potential pharmacological target that might help preserve visual acuity in nAMD. OCT imaging of the retinal and subretinal findings at the site of fibrosis or atrophy could also clarify disparate and common pathways of morphology change leading to greater understanding of the pathophysiology of the lesion response at two years. Therefore, in this study we analyzed data from eyes with areas designated on CP/FA as geographic atrophy, non-geographic atrophy, fibrous scar or non-fibrous scar in the macula at the two-year visit in the CATT. To extract this information, we used previously published methods to register and assess OCT features within areas given the above designations based on CP/FA.

## Methods:

The participants in and methods of CATT have been described in a previous publication[13] and at the ClinicalTrials.gov website (NCT00593450). Enrollment extended across 43 clinical centers in the U.S. from February 2008 to December 2009. The study was approved by an institutional review board associated with each center, and was compliant with the Health Insurance Portability and Accountability Act regulations. The study was performed in accordance with the tenets of the Declaration of Helsinki. All participants provided written informed consent.

The image analysis methods have been published previously.[13] Briefly, the CATT participants had bilateral stereo CP, stereo FA and time domain optical coherence tomography at baseline. CP, FA and OCT were repeated at 1, 2 and 5 years, and spectral domain (SD) OCT was captured in many of the CATT participants after the year 1 visit. Thus, year 2 (104 week visit) scans were either captured with TD OCT or SDOCT. Only SDOCT scans were used in this study because of their denser pattern of capture and higher resolution than TDOCT. The SDOCT systems included Cirrus (Carl Zeiss Meditec, California) and Spectralis (Heidelberg Engineering, Germany), with scan patterns as previously reported[13]. Photographic images were evaluated by the CATT Fundus Photography Reading Center (University of Pennsylvania, Philadelphia, PA) and OCT images were evaluated by certified readers at the CATT OCT Reading Center (Duke University, Durham, NC). The location of specific SDOCT features was delineated by readers at Dr. Toth's Duke Advanced Research in SS/SDOCT Imaging (DARSI) Laboratory (Duke University). Readers at each reading center were masked to the assessment from the other reading center[13].

Four main features identifiable on stereo CP/FA images of eyes treated with anti-VEGF agents were selected for in-depth evaluation based on the prior Photographic Reading Center definitions: 1) geographic atrophy (GA), 2) non-geographic atrophy (NGA), 3) fibrotic scar

(FS), and 4) non-fibrotic scar (NFS)[13] (definitions in Table 1). While we recognize the controversy over the use of the term GA for macular atrophy after nAMD treatment, we retained the GA terminology because our original categorization of atrophic findings into two mutually exclusive lesion components, GA or NGA, employed this language. Seventy eyes of 70 participants at the 104-week CATT visit with one or more of these features present on CP/FA and with SDOCT scans were selected by the CATT Coordinating Center using stratified sampling to get a representative sample of images with these features present at fovea or outside of fovea. Because of the complexity of the overlay analyses, we did not include nAMD lesions without at least one of these components. It was not possible to analyze photographic or OCT images on two of the 70 eyes because of inadequate image quality.

To analyze photographs, CP/FA lesion components were marked within a 6-mm circular region centered on the fovea. To analyze SDOCT images, retinal and subretinal features were marked, and retinal and subretinal boundaries were segmented to determine lesion thicknesses across the SDOCT volume scans. These markings and the methods for image overlay are detailed by Toth et al[13] and summarized below.

For CP/FA, graders delineated the total CNV lesion (TCNVL) and 10 component morphological features as previously described[13] (Figure 1): CNV, hemorrhage, fibrotic scar, non-fibrotic scar, serous pigment epithelial detachment (SPED), blocked fluorescence, geographic atrophy (GA), non-geographic atrophy (NGA), retinal angiomatous proliferation (RAP), and retinal pigment epithelial tear (RPE tear). Each morphology was outlined with a unique color and each of the 10 components was exclusive at any single location, so that a site could not be assigned more than one component. In addition to lesion components, we designated “non-lesion” regions as CP/FA or OCT areas without marked lesion components.

For SDOCT, Readers used proprietary software, Duke OCT Retinal Analysis Program (DOCTRAP) Marking Code Version 61.4.2 developed in MATLAB R2012a (MathWorks, Natick, Massachusetts) to mark the foveal center, optic disc center, and the lateral extent of 11 morphologic features within every B-scan of the macular volumes as previously described (Figure 1): intraretinal fluid (IRF), outer retinal tubulation (ORT; hyper-reflective rosettes, similar to and thought to reflect early development of ORT, while marked separately, were combined within the category “ORT” for this analysis), subretinal fluid (SRF), subretinal highly reflective material (SHRM), non-drusenoid pigment epithelial detachment (PED), indistinguishable SHRM/PED, sub-RPE fluid and photoreceptor layer thinning. We also marked RPE atrophy with choroidal hyper-transmission (called RPE atrophy) which could be present with or without overlying lesion material. While most SDOCT features could be co-localized at the same pixel location (e.g. IRF, SHRM and PED), by definition, RPE atrophy without overlying lesion was mutually exclusive with all of the following: SHRM, PED, Indistinguishable SHRM/PED, Sub RPE-fluid, and RPE atrophy with overlying lesion material. Thickness of the RPE+drusen+lesion complex (RPEDLC, RPE plus all drusen material, whether above or below the RPE plus all subretinal/sub-RPE lesion components plus subretinal/sub-RPE fluid) was extracted from semi-automated segmentation of scans across a 5-mm diameter circular region centered on the fovea[14]. Thickness of the neurosensory retina (NSR, retina without subretinal lesion

complex or RPE) was also measured across this region. Because of the variable thickness of the neurosensory retina across the fovea, the thickness was reported relative to the mean thickness at that foveal location, based on a dataset from 115 eyes of 119 control participants, mean age 67 (range 51 to 83 years) without AMD from the AREDS2 ancillary SDOCT study[15].

Photographic and OCT overlay images were manually registered and pixels were interpolated. CP/FA and OCT markings were compared side-by-side, and overlays of the SDOCT and CP/FA data were extracted pixel by pixel using custom MATLAB software with a graphic user interface (CATTREG V2.9, developed in the DARSI Laboratory by CAT, VT and SJC) for a 5-mm diameter circular region. The software produced a dataset containing each pixel's location on a standardized grid, and for each pixel, a binary value for presence of each OCT feature or CP/FA component, and OCT thickness measurements. We analyzed the frequency of OCT features within the CP/FA components of each of the 68 study eyes. We also evaluated the percentage of pixels covered by OCT features within the total pixel area of each of the four distinct CP/FA lesion components and also the area outside of the CP/FA total CNV lesion for each eye. To evaluate the relationship between layer thicknesses and qualitative SDOCT morphology within the CP/FA components, we determined the NSR or RPEDLC thickness for the pixels of selected OCT features within the four CP/FA components

### STATISTICAL ANALYSIS:

We compared the frequency of the OCT features within the CP/FA components in eyes using Fisher's exact tests. We also determined the median and quartiles of the percentage of pixels containing OCT features per designated CP/FA component area in each eye for which OCT data were available. We subsequently determined the percentage of each of the four CP/FA component pixels that was occupied by different OCT features alone and in combination. We compared the median values between CP/FA features using Kruskal-Wallis tests. We also calculated the mean thickness and volume of the RPEDLC for pixels designated as each of the four CP/FA features and for the non-feature region, and compared them using Kruskal-Wallis tests.

## Results:

Within the 68 eyes of 68 participants at the 104 week CATT visit, the four CP/FA lesion components were represented as follows: 25 eyes had GA, 44 eyes had NGA, 26 eyes had FS, and 7 eyes had NFS. More than one CP/FA lesion component was present in over 1/3 of the eyes. When present, GA, NGA, FS and NFS comprised a median of 17%, 28%, 12% and 2%, respectively, of the 5-mm diameter circular region area.

The frequency of OCT features within the CP/FA components and within the areas outside of the CP/FA-designated total CNV lesion components is shown in Table 1 in the rows labelled "eyes". The percentage of pixels covered by OCT features within the total pixel area of each of the four distinct CP/FA lesion components and within the areas outside of the CP/FA total CNV lesion for each eye is shown in Table 1 in the rows labelled "% pixels". The thicknesses of the RPE+drusen+lesion complex and of the variance in neurosensory

retinal thickness relative to normative data for aged eyes are shown in Figures 2 and 3. These findings are addressed in detail below. A cross tabulations between the different OCT features at the same pixel location is shown in Table 2 (available at http://www.ophthalmology-retina.org).

OCT features of RPE atrophy with choroidal hyper-transmission included areas with and without residual lesion material. The majority of RPE atrophy without overlying lesion was found almost exclusively in GA: it was present in 80% of GA eyes and covered a median of 25% of GA pixels in those eyes. The next closest amount was in NGA where it covered a median of 1% of pixels in 32% of NGA eyes; it was rarely found in NFS and was not present in eyes with FS (Table 1). In contrast, RPE atrophy with overlying lesion was present in areas of atrophy and of scar; it was present in 100% of eyes with GA, 95% with NGA, 88% with FS and 57% with NFS, respectively. Notably, it covered an additional median 52% of GA pixels, 22% of NGA pixels, 46% of FS pixels and 24% of NFS pixels in eyes containing these components. Furthermore, within GA, the mean (SD) thickness of the RPE+drusen+lesion complex was different between areas of RPE atrophy with overlying lesion (51.4±27 microns) versus RPE atrophy without overlying lesion (27.2 ±9 microns, $p<0.001$). Within FS the mean thickness of the RPE+drusen+lesion complex was not different between areas with and without RPE atrophy with choroidal hyper-transmission (140±64 versus 153±90 microns, $p=0.23$), all of which had residual lesion present.

Photoreceptor layer thinning visible to the OCT reader extended over a median of 76% of pixels designated as RPE atrophy with choroidal hyper-transmission: the photoreceptor loss covered a median of 95% of pixels over RPE atrophy without an overlying lesion and 73% over RPE atrophy with an overlying lesion. While the frequency of photoreceptor loss matched that of the RPE atrophy, photoreceptor loss extended across a larger median percentage of pixels than did RPE atrophy for all lesion components: a median of 85% (photoreceptor loss) versus 75% (RPE atrophy) for the GA area, 42% versus 22% for the NGA area, 59% versus 46% for fibrotic scar area, and 33% versus 24% for the non-fibrotic scar area (Table 1). The qualitative finding of photoreceptor loss by Readers was not distinguished by deviation in neurosensory retinal thickness relative to normative data for aged eyes except in those with GA. Across GA, mean NSR deviation relative to normal was −22±35microns (Figure 3). Outer retinal tubulations, thought to represent photoreceptor degeneration, were uncommon in NFS lesions (14%) and present in similar frequency in GA, NGA and FS (36 to 48%), although they involved minimal lesion component area (medians were ≤4% of the area).

An OCT subretinal lesion feature (SHRM, PED, or indeterminate SHRM or PED) was present within the lesion component in 80% of eyes with GA, in 95% with NGA and in 100% with NFS and FS and involved a median of 31% of the GA area, 42% of the NGA area, 85% of the NFS area and 92% of the FS area per eye, respectively (Table 1). The CP/FA lesion components with greater percentage of OCT-determined subretinal lesion feature area, also had greater mean (± standard deviation) thickness of the RPE + drusen + lesion complex (RPEDLC): 48 (± 25) microns for GA, 61 (± 35) microns for NGA, 83 (± 17) for NFS, 151 (± 74) microns for FS and 33 (± 6) microns for non-lesion areas, respectively ($p<0.001$; Figure 2). In pixels designated as subretinal lesion by OCT grading,

the mean RPEDLC thickness was not significantly different whether they were located in areas of NGA (80±37 microns) or GA (73±22, p=0.26). Because so much of the NFS and FS lesion area was covered by subretinal lesion features (85% and 92% respectively), there was little difference between the mean RPEDLC over the entire component versus in areas of OCT-determined subretinal lesion.

Among subretinal lesion features on OCT, the total component area covered by SHRM was greatest in FS (71%) and much lower in GA, NFS, and NGA (27%, 16% and 8%, respectively); whereas the area covered by PED was greater in both FS and NFS (80% and 72%) and lower in NGA and GA (32% and 18%). While SHRM and PED features could overlap within these component areas, the relative total pixel area occupied by PED was greater than that occupied by SHRM in areas of NFS and NGA. Although the indeterminate SHRM/PED feature was present in 35-52% of component lesions, it extended across only 2 to 9% of any of the component areas.

Fluid was commonly identified on OCT across all four components (frequency from 43% to 73%). The fluid, however, covered minimal lesion component areas 2% to 6% except in FS for which it involved a median of 14% of lesion area. The fluid area in FS lesions was predominantly sub-RPE fluid which covered a median of 26% of the FS pixels per eye in contrast to IRF and SRF which covered a median of 4% of the FS pixels per eye. IRF covered a median of 13% of NFS area, and SRF covered a median of 9% of the NGA area. The remaining fluid involved a median of ≤3% of lesion areas.

All 68 eyes had areas with OCT features that were designated outside the CP/FA designated total CNV lesion area. Analysis of these areas showed that while almost every SDOCT feature was present within the non-lesion area, they comprised less than 2% of the area except for the following components which were found most typically near the margin of the CP/FA designated lesion: photoreceptor layer loss, found in 65 eyes (96%), covered a median of 7% of the non-lesion area per eye; PED, in 64 eyes (94%), covered a median of 3% of the area; and RPE atrophy with choroidal hyperreflectance and overlying material, in 58 eyes (85%), extended across a median of 3% of the area. All of the designated OCT features were absent across a median of 27% of NGA, 20% of NFS, 3% of the FS and 6% of the GA component pixels per eye, and across a median of 87% of the non-lesion pixels per eye.

From a cross-tabulation between the OCT features per overlay pixel (Table 2, available at http://www.ophthalmology-retina.org), we identified that subretinal lesion (SHRM, PED or indeterminate SHRM/PED) co-localized with 68.6% of any fluid pixels: 99.5% of subRPE fluid pixels, 79.2% of the IRF pixels, and 56% of subretinal fluid. Distinct subretinal lesion (SHRM, PED or indeterminate SHRM/PED) was present in 51.5% of RPE atrophy with overlying lesion. Photoreceptor loss shared 72% of pixels with RPE atrophy with overlying lesion and 94% of RPE atrophy without overlying lesion.

## Discussion

Researchers have used OCT to compare morphological features and to assess quantitatively retinal and subretinal lesion volumes in nAMD. The majority of analyses of OCT features have been recorded per macula or per a smaller central region of the macula (e.g. central subfield or foveal center) or have measured the largest lateral dimension of a feature[16, 17]. Similarly, thickness assessments have typically used bulk measurements per macula, single measurements at the foveal center, or areas or volumes measured within different diameter circles centered on the fovea[18–21]. Some studies have evaluated co-localized fluid and PED featured in nAMD[22]. In this study, we report the first analysis of OCT features by precise macular location and extent relative to components identified on CP/FA.

After two years of anti-VEGF treatment for nAMD in the CATT, the distribution of eleven optical coherence tomography (OCT)-based features across macular areas of CP/FA-designated FS, NFS, GA, NGA and no-lesion component, reveals disparate and common retinal and subretinal morphologic features. When one considers the OCT findings across these four categories, there is a continuum of RPE and photoreceptor atrophy across all lesions. RPE atrophy and photoreceptor layer thinning is common not only in areas of macular atrophy but in areas of fibrotic scar; not surprisingly, the greatest atrophy was observed within GA areas, however this was followed by FS in which the median percent of RPE atrophy area per affected eye was greater than in NGA and NFS.

The difference in CP/FA appearance seemed to be impacted most by the thickness and extent of the subretinal lesion complex. Fibrosis was seen on CP/FA when the subretinal lesion complex was thicker and more extensive. While RPE atrophy with overlying lesion did not distinguish FS (median 46% of pixels in 88% of FS eyes) from GA (52% of pixels in 100% of GA eyes), RPE atrophy without lesion was almost exclusively in areas that appeared as GA on CP/FA. The difference in CP/FA appearance was influenced less by photoreceptor atrophy which was most profound in GA (median pixel area of 85%), less in regions with FS (59%) and lower in regions with NGA and NFS (median pixel areas 42% and 33% respectively). The extent of RPE atrophy with choroidal hyper-transmission, photoreceptor loss and degenerative change (outer retinal tubulation) in FS was striking in that it was similar to or more extensive than in NGA. While photoreceptor loss has been documented over chronic fibrosis, the extent of RPE loss and choroidal hyper-transmission has not been as clearly categorized.

Subretinal lesion components were common in areas of scar, but were also present in nearly 1/3 or more of areas of macular atrophy. The traditional description of GA based on CP/FA intends to describe areas with loss of photoreceptors, RPE and choriocapillaris and without subretinal tissue and fluid. During chronic multi-year anti-VEGF treatments, areas of similar appearing sharply demarcated atrophy on CP/FA may be found within the bed of the previously active CNV complex, or in dissociated areas. In the former location, these have been recognized to contain residual subretinal components reflective of prior CNV in that location[23]. In this study, while areas that appear as “GA” on CP/FA after 2 years of anti-VEGF treatment have loss of RPE cell pigment (resulting in choroidal hyper-transmission) and photoreceptor loss, they also have retained subretinal material, though thinner than that

in fibrotic scar. In the GA regions, while a median of 25% of pixels had RPE atrophy with choroidal hyper-transmission and no overlying lesion, a median of 31% of pixels contained subretinal lesion components. The median thickness of the RPEDLC in those GA (and NGA) areas with subretinal lesion components were greater not only than in area of GA without subretinal lesion components but also than in non-lesion areas. The thicker material here, in NGA or even in FS may contribute to further development of atrophy as noted in a prior CATT longitudinal analysis[7].

Atrophy of photoreceptors and RPE appears to be common across large areas of both GA and FS and beyond the clinically recognized lesion margins, and less so in NGA and NFS. While areas identified as FS on CP/FA after 2 years of anti-VEGF treatment retain thicker subretinal material across the greatest lesion area, they also have loss of RPE and photoreceptors. Notably in FS, choroidal hyper-transmission with RPE atrophy was found in a median of 46% of FS pixels per eye, and photoreceptor layer thinning extended across a median of 59% of FS pixels per eye. Thus, although there is a distinct difference between FS and GA in the area and thickness of retained subretinal lesion material, they share high rates of photoreceptor loss (median 85% of area in GA and 59% in FS) and increased choroidal hypertransmssion with loss of RPE (median 75% of area in GA and 46% in FS). Both NGA and NFS had lesser extents of photoreceptor atrophy and choroidal hyper-transmission, Table 1). These morphologies may help to explain the poorer visual acuities found with increased duration of treatment in eyes with atrophy and FS[7]. A related finding from CATT was poorer visual acuity with loss of the ellipsoid zone at the foveal center over areas of SHRM, though choroidal hyper-transmission was not analyzed in that substudy[24]. By identifying these common retinal and subretinal anatomic elements that help to explain visual acuity loss in both fibrosis and atrophy, we point to the potential value of OCT endpoints when applying therapeutics to preserve or recover RPE and photoreceptors in nAMD.

Areas designated as NGA demonstrated types and distribution of OCT features that were quite different from GA. Of eyes with NGA when compared to GA, there were a smaller percentage with choroidal hyper-transmission associated and RPE atrophy without overlying subretinal lesion material, an appearance that covered very tiny areas of the NGA (a median of 1% of pixels). In these eyes the median percentage with choroidal hyper-transmission associated and RPE atrophy with overlying subretinal lesion material was also lower than that observed in GA and in FS. As expected, subretinal lesions on OCT (either PED, SHRM or indeterminate SHRM/PED) were slightly more extensive in NGA than in GA and the median RPEDLC thickness in NGA was comparable to that in GA and again, greater than in non-lesion areas. The distinction between NGA and GA on CP/FA may also be due in part to the lesser extent of photoreceptor loss in NGA, which is about half of that in GA. Percent area of photoreceptor loss was also lower than in FS (59%). This finding helps to explain the observation that eyes with subfoveal NGA have better visual acuity than eyes with subfoveal FS or GA but not as good as eyes without subfoveal lesions at 2 and 5 years[25].

In CATT at 2 years, the NFS were flat and small lesions with well-circumscribed areas of pigmentation[1] (comprising only 2% of a central 6 mm ring area in this study). Although they had a high percentage of area covered by lesion complex, perhaps due to their small size,

they retained RPE pigmentation (only 24% of pixels with choroidal hyper-transmission with RPE atrophy), had thinner RPEDLC, and had less photoreceptor layer thinning (33% of pixels). This helps to explain the retained visual acuity documented at 2 years of treatment in eyes with subfoveal NFS in CATT[7].

Taken together, our observations support the importance of OCT imaging to capture the full extent of retinal and residual nAMD lesion features and atrophy, during treatment of nAMD, especially for clinical trials that relate morphologic features to functional outcomes. The range of morphology present within areas designated on CP/FA as GA point to the limitations in the use of that vary general classification [26]. While it is important to document post-treatment presence or absence and thickness of subretinal lesion complex as this relates to extent of photoreceptor loss, it is also important to recognize that the extent of photoreceptor loss is usually greater than the area of choroidal hyper-transmission within the FS, NFS, NGA and even GA. Photoreceptor loss extended across a median of 7% of non-lesion areas in 96% of eyes. Thus, photoreceptor loss alone (defined at the Classification of Atrophy Meeting as incomplete outer retinal atrophy and complete outer retinal atrophy[27]) is an important OCT variable, as this information would not be captured with designations based on choroidal hyper-transmission with RPE and outer retinal atrophy[27]. This information will be especially important in studies of therapies with a goal of photoreceptor salvage or regeneration.

Our study has limitations. The significance is unclear of differences between the CP/FA component groups, which includes the NFS category which had a small number of eyes (n=7); when analyses were calculated without inclusion of NFS, there was minimal change in p-values and significance of the findings did not change. We could not consider the contribution of choroidal thickness in this analysis as it was not consistently imaged at these study visits[3]. Multimodal imaging is useful to identify polypoidal disease and components such as reticular drusen, vitelliform and other deposits[28]; and OCT angiography has been proposed to provide delineation of risk groups in nAMD[29–31]. This study did not address infrared or OCT angiographic imaging.

Future longitudinal analyses will be important to derive information on the precursor retinal and subretinal lesion features in areas of macular atrophy, choroidal hyper-transmission and RPE atrophy, and fibrosis at year 2 and their outcomes at year 5. It will be useful to perform a longitudinal study of all components of these lesions, to identify the pre-treatment morphology of neovascular lesions that preceded these various features and the subsequent evolution of these features several years later. This type of analysis will be especially important in light of the poorer visual outcomes in eyes with scar or atrophy and the progressive appearance of such areas after longer periods of anti-VEGF treatment for nAMD.

## Supplementary Material

Refer to Web version on PubMed Central for supplementary material.

## Acknowledgments

**Funding:** Supported by cooperative agreements U10 EY017823, U10 EY017825, U10 EY017826, U10 EY017828, and U10 EY023530 from the National Eye Institute, National Institutes of Health, Department of Health and Human Services, Bethesda, Maryland. The funding organization participated in the design and conduct of the study and review of the manuscript.

## Abbreviations and acronyms that are used in the manuscript:

| | |
|---|---|
| **AMD** | age-related macular degeneration |
| **CATT** | Comparison of Age-related Macular Degeneration Treatments Trials |
| **CP** | color photograph |
| **FA** | fluorescein angiography |
| **FS** | fibrotic scar |
| **GA** | geographic atrophy |
| **IRF** | intraretinal fluid |
| **nAMD** | neovascular AMD |
| **NFS** | non-fibrotic scar |
| **NGA** | non-geographic atrophy |
| **OCT** | optical coherence tomography |
| **RPE** | retinal pigment epithelium |
| **RPEDLC** | RPE+drusen+lesion complex |
| **SDOCT** | spectral domain optical coherence tomography |
| **SRF** | subretinal fluid |
| **VEGF** | vascular endothelial growth Factor |

## References:

1. Daniel E, Toth CA, Grunwald JE, et al. Risk of scar in the comparison of age-related macular degeneration treatments trials. Ophthalmology 2014;121(3):656–66. [PubMed: 24314839]
2. Sadda SR, Tuomi LL, Ding B, et al. Macular Atrophy in the HARBOR Study for Neovascular Age-Related Macular Degeneration. Ophthalmology 2018.
3. Abdelfattah NS, Al-Sheikh M, Pitetta S, et al. Macular Atrophy in Neovascular Age-Related Macular Degeneration with Monthly versus Treat-and-Extend Ranibizumab: Findings from the TREX-AMD Trial. Ophthalmology 2017;124(2):215–23. [PubMed: 27863845]
4. Grunwald JE, Pistilli M, Daniel E, et al. Incidence and Growth of Geographic Atrophy during 5 Years of Comparison of Age-Related Macular Degeneration Treatments Trials. Ophthalmology 2017;124(1):97–104. [PubMed: 28079023]
5. Grunwald JE, Daniel E, Huang J, et al. Risk of geographic atrophy in the comparison of age-related macular degeneration treatments trials. Ophthalmology 2014;121(1):150–61. [PubMed: 24084496]

6. Jaffe GJ, Martin DF, Toth CA, et al. Macular morphology and visual acuity in the comparison of age-related macular degeneration treatments trials. Ophthalmology 2013;120(9):1860–70. [PubMed: 23642377]
7. Daniel E, Pan W, Ying GS, et al. Development and Course of Scars in the Comparison of Age-related Macular Degeneration Treatments Trials. Ophthalmology 2018.
8. Sharma S, Toth CA, Daniel E, et al. Macular Morphology and Visual Acuity in the Second Year of the Comparison of Age-Related Macular Degeneration Treatments Trials. Ophthalmology 2016;123(4):865–75. [PubMed: 26783095]
9. Sarwar S, Clearfield E, Soliman MK, et al. Aflibercept for neovascular age-related macular degeneration. Cochrane Database Syst Rev 2016;2:CD011346. [PubMed: 26857947]
10. Ying GS, Kim BJ, Maguire MG, et al. Sustained visual acuity loss in the comparison of age-related macular degeneration treatments trials. JAMA Ophthalmol 2014;132(8):915–21. [PubMed: 24875610]
11. Berg K, Roald AB, Navaratnam J, Bragadottir R. An 8-year follow-up of anti-vascular endothelial growth factor treatment with a treat-and-extend modality for neovascular age-related macular degeneration. Acta Ophthalmol 2017;95(8):796–802. [PubMed: 28926190]
12. Chakravarthy U, Harding SP, Rogers CA, et al. Alternative treatments to inhibit VEGF in age-related choroidal neovascularisation: 2-year findings of the IVAN randomised controlled trial. Lancet 2013;382(9900):1258–67. [PubMed: 23870813]
13. Toth CA, Tai V, Chiu SJ, et al. Linking OCT, Angiographic, and Photographic Lesion Components in Neovascular Age-Related Macular Degeneration. Ophthalmology Retina 2018;2(5):481–93.
14. Chiu SJ, Izatt JA, O'Connell RV, et al. Validated automatic segmentation of AMD pathology including drusen and geographic atrophy in SD-OCT images. Invest Ophthalmol Vis Sci 2012;53(1):53–61. [PubMed: 22039246]
15. Farsiu S, Chiu SJ, O'Connell RV, et al. Quantitative classification of eyes with and without intermediate age-related macular degeneration using optical coherence tomography. Ophthalmology 2014;121(1):162–72. [PubMed: 23993787]
16. Waldstein SM, Simader C, Staurenghi G, et al. Morphology and Visual Acuity in Aflibercept and Ranibizumab Therapy for Neovascular Age-Related Macular Degeneration in the VIEW Trials. Ophthalmology 2016;123(7):1521–9. [PubMed: 27157149]
17. Wintergerst MWM, Schultz T, Birtel J, et al. Algorithms for the Automated Analysis of Age-Related Macular Degeneration Biomarkers on Optical Coherence Tomography: A Systematic Review. Transl Vis Sci Technol 2017;6(4):10.
18. Vogl WD, Waldstein SM, Gerendas BS, et al. Analyzing and Predicting Visual Acuity Outcomes of Anti-VEGF Therapy by a Longitudinal Mixed Effects Model of Imaging and Clinical Data. Invest Ophthalmol Vis Sci 2017;58(10):4173–81. [PubMed: 28837729]
19. Bogunovic H, Waldstein SM, Schlegl T, et al. Prediction of Anti-VEGF Treatment Requirements in Neovascular AMD Using a Machine Learning Approach. Invest Ophthalmol Vis Sci 2017;58(7): 3240–8. [PubMed: 28660277]
20. Choi CS, Zhang L, Abramoff MD, et al. Evaluating Efficacy of Aflibercept in Refractory Exudative Age-Related Macular Degeneration With OCT Segmentation Volumetric Analysis. Ophthalmic Surg Lasers Imaging Retina 2016;47(3):245–51. [PubMed: 26985798]
21. Amoaku WM, Chakravarthy U, Gale R, et al. Defining response to anti-VEGF therapies in neovascular AMD. Eye (Lond) 2015;29(10):1397–8. [PubMed: 26446737]
22. Klimscha S, Waldstein SM, Schlegl T, et al. Spatial Correspondence Between Intraretinal Fluid, Subretinal Fluid, and Pigment Epithelial Detachment in Neovascular Age-Related Macular Degeneration. Invest Ophthalmol Vis Sci 2017;58(10):4039–48. [PubMed: 28813577]
23. Holz FG, Sadda SR, Staurenghi G, et al. Imaging Protocols in Clinical Studies in Advanced Age-Related Macular Degeneration: Recommendations from Classification of Atrophy Consensus Meetings. Ophthalmology 2017;124(4):464–78. [PubMed: 28109563]
24. Willoughby AS, Ying GS, Toth CA, et al. Subretinal Hyperreflective Material in the Comparison of Age-Related Macular Degeneration Treatments Trials. Ophthalmology 2015;122(9):1846–53 e5. [PubMed: 26143666]

25. Comparison of Age-related Macular Degeneration Treatments Trials Research G, Maguire MG, Martin DF, et al. Five-Year Outcomes with Anti-Vascular Endothelial Growth Factor Treatment of Neovascular Age-Related Macular Degeneration: The Comparison of Age-Related Macular Degeneration Treatments Trials. Ophthalmology 2016;123(8):1751–61. [PubMed: 27156698]

26. Schmitz-Valckenberg S, Sadda S, Staurenghi G, et al. Geographic Atrophy: Semantic Considerations and Literature Review. Retina 2016;36(12):2250–64. [PubMed: 27552292]

27. Sadda SR, Guymer R, Holz FG, et al. Consensus Definition for Atrophy Associated with Age-Related Macular Degeneration on OCT: Classification of Atrophy Report 3. Ophthalmology 2018;125(4):537–48. [PubMed: 29103793]

28. Kuroda Y, Yamashiro K, Tsujikawa A, et al. Retinal Pigment Epithelial Atrophy in Neovascular Age-Related Macular Degeneration After Ranibizumab Treatment. Am J Ophthalmol 2016;161:94–103 e1. [PubMed: 26432927]

29. Kuehlewein L, Dustin L, Sagong M, et al. Predictors of Macular Atrophy Detected by Fundus Autofluorescence in Patients With Neovascular Age-Related Macular Degeneration After Long-Term Ranibizumab Treatment. Ophthalmic Surg Lasers Imaging Retina 2016;47(3):224–31. [PubMed: 26985795]

30. Lindner M, Fang PP, Steinberg JS, et al. OCT Angiography-Based Detection and Quantification of the Neovascular Network in Exudative AMD. Invest Ophthalmol Vis Sci 2016;57(14):6342–8. [PubMed: 27898979]

31. Ichiyama Y, Sawada T, Ito Y, et al. Optical Coherence Tomography Angiography Reveals Blood Flow in Choroidal Neovascular Membrane in Remission Phase of Neovascular Age-Related Macular Degeneration. Retina 2017;37(4):724–30. [PubMed: 28248824]

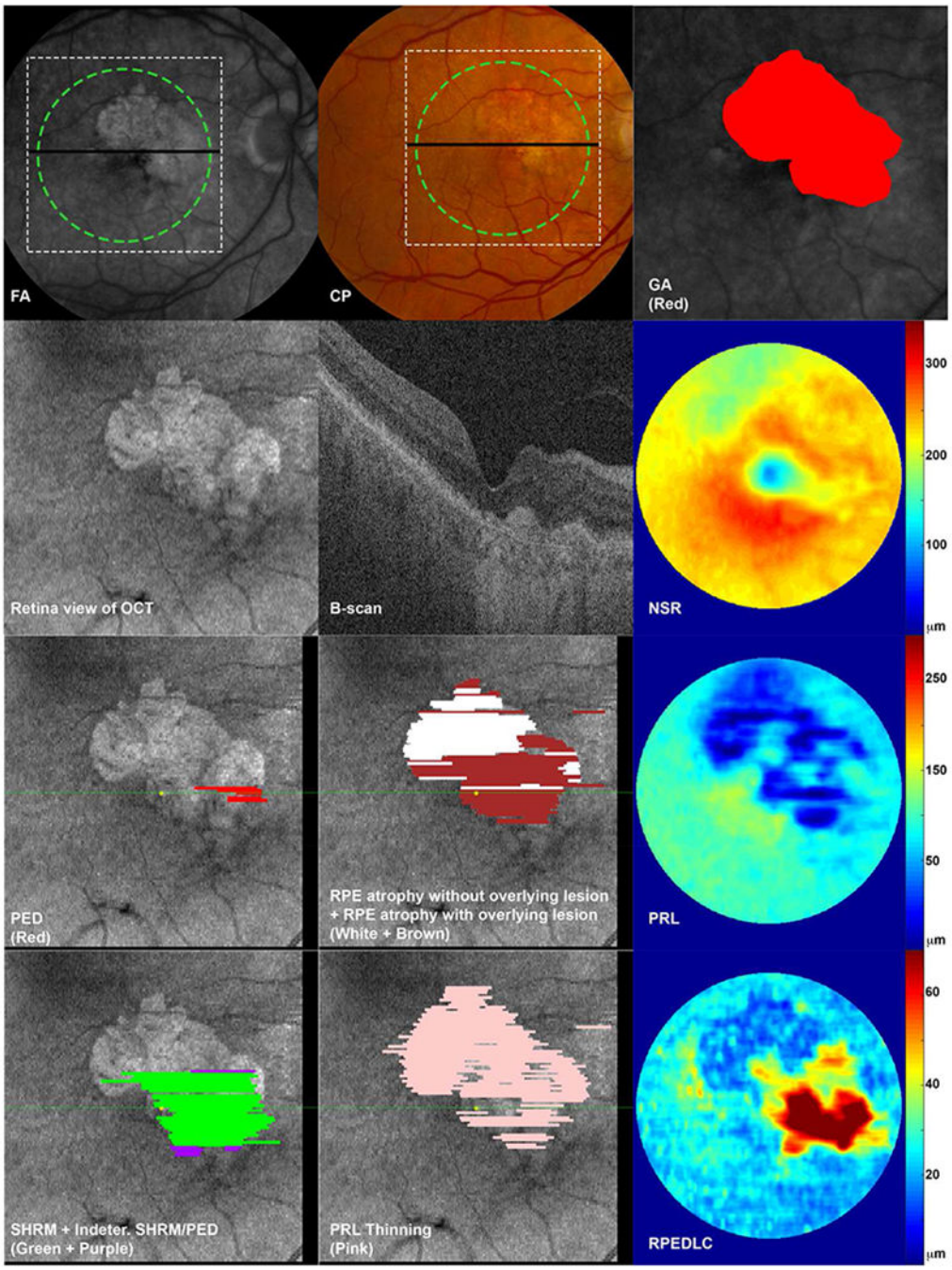


**Figure 1.**

Overlay of color photographic/fluorescein angiographic (CP/FA) designated characteristics and optical coherence tomography (OCT) designated features and thicknesses on aligned macular regions at the year 2 visit in CATT for an eye with predominant CP/FA designated geographic atrophy and predominant CP/FA designated fibrotic scar. GA = geographic atrophy, NSR = neurosensory retina, PED = non-drusenoid pigment epithelial detachment, RPE = retinal pigment epithelium, PRL = photoreceptor layer, SHRM = subretinal highly reflectively material, RPEDLC = RPE + drusen + lesion complex.

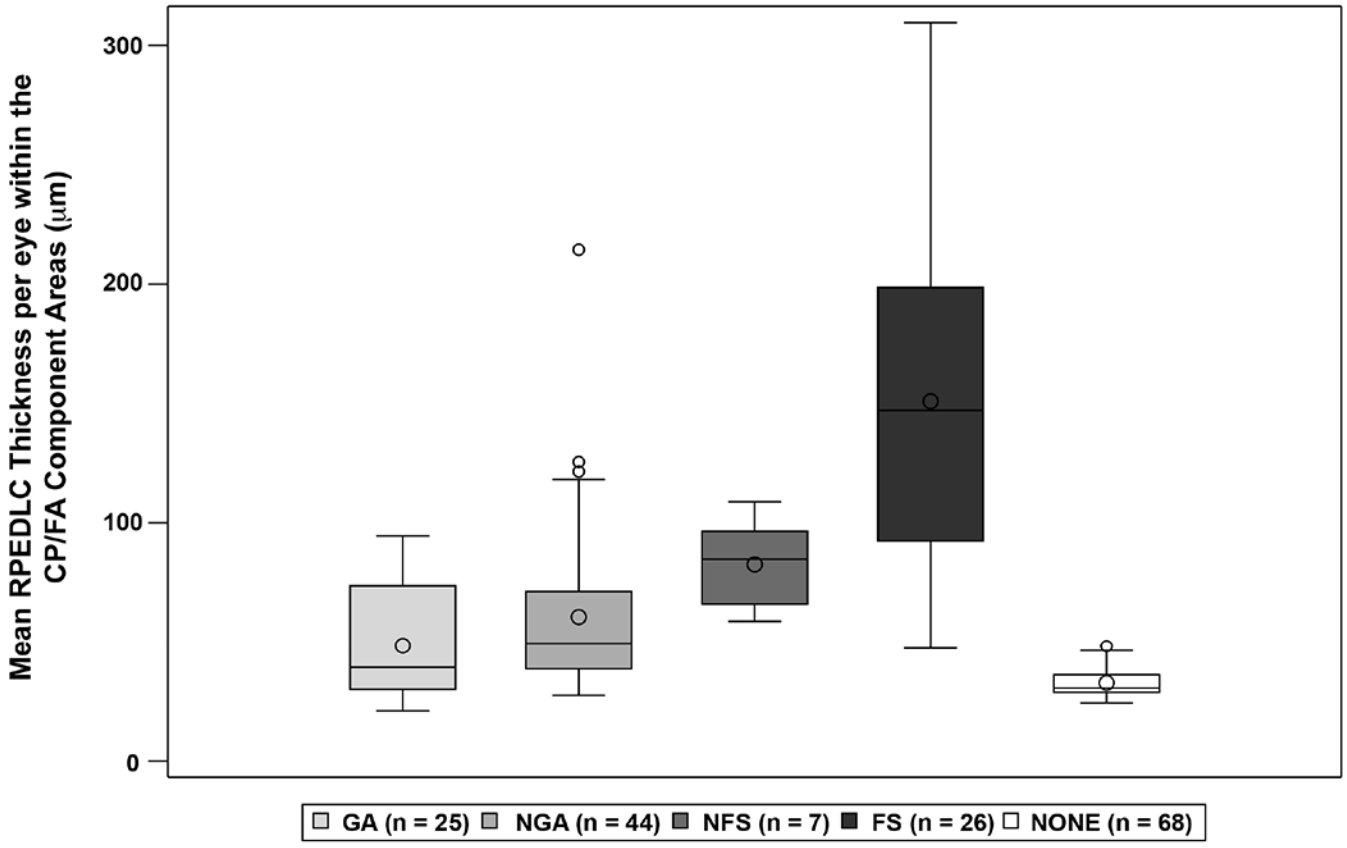


**Figure 2.**

Distribution among eyes of the mean thickness on optical coherence tomography (OCT) of the retinal pigment epithelium + drusen + lesion complex for the pixels within each color photograph (CP) /fluorescein angiographic (FA) component: GA = geographic atrophy, NGA = non-geographic atrophy, NFS = non-fibrotic scar, FS= fibrotic scar and NONE = macular areas without any lesion components. RPEDLC = retinal pigment epithelium + drusen + lesion complex. Box and whisker plots: Box upper and lower edges correspond to the 75th and 25th percentiles, respectively. Within the box, the circle corresponds to the mean value and the line corresponds to the 50th percentile (median). Ends of whiskers correspond to the lowest score within 1.5 times the interquartile range of the 25th percentile and the highest score within 1.5 times the interquartile range of 75th percentile. Each circle outside of the whiskers corresponds to outliers of the score.

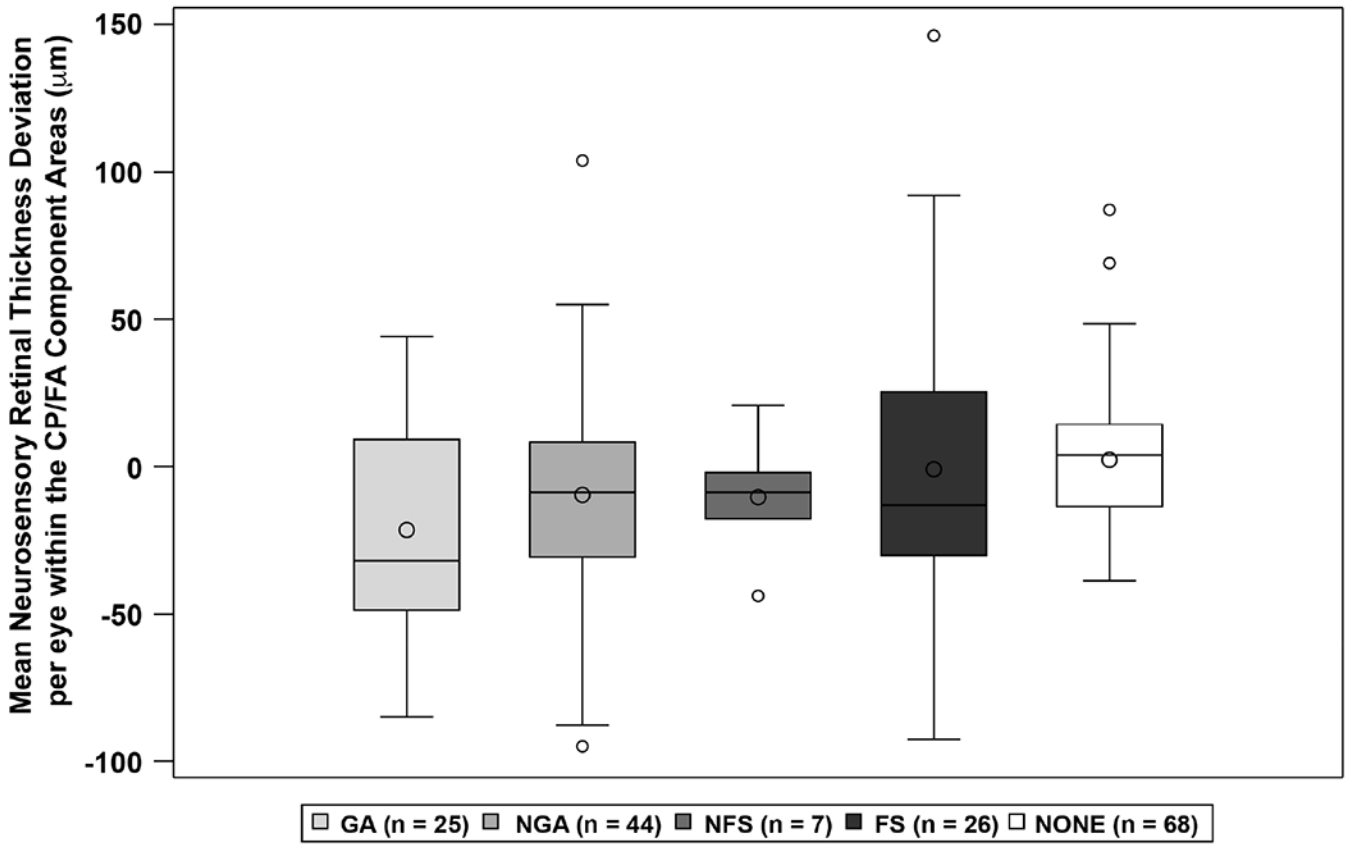


**Figure 3.**

Distribution among eyes of the mean retinal thickness on optical coherence tomography (OCT) for the pixels within each color photograph (CP) /fluorescein angiographic (FA) component: GA = geographic atrophy, NGA = non-geographic atrophy, NFS = non-fibrotic scar, FS= fibrotic scar and NONE = macular areas without any lesion components. Box and whisker plots: Box upper and lower edges correspond to the 75th and 25th percentiles, respectively. Within the box, the circle corresponds to the mean value and the line corresponds to the 50th percentile (median). Ends of whiskers correspond to the lowest score within 1.5 times the interquartile range of the 25th percentile and the highest score within 1.5 times the interquartile range of 75th percentile. Each circle outside of the whiskers corresponds to outliers of the score.

**Table 1:**

Frequency and median of the percentage of pixels of optical coherence tomography (OCT) features within each color photographic (CP)/fluorescein angiographic (FA) component of 68 study eyes.

| OCT feature | | CP/FA component | | | | p | No CP/FA component |
|---|---|---|---|---|---|---|---|
| | | Geographic Atrophy (GA) n=25 | Non-Geographic Atrophy (NGA) n=44 | Non-Fibrotic Scar (NFS) n=7 | Fibrotic Scar (FS) n=26 | | Macular area outside total CNV lesion, n=68 |
| | eyes containing any pixels of OCT feature | n (%) | n (%) | n (%) | n (%) | | n (%) |
| | percent of pixels with OCT features within the CP/FA component* | Median (25%, 75%) | Median (25%, 75%) | Median (25%, 75%) | Median (25%, 75%) | | Median (25%, 75%) |
| **RPE Atrophy** with choroidal hypertransmission | eyes | 25 (100%) | 42 (95%) | 4 (57%) | 23 (88%) | 0.005 | 58 (85%) |
| | % pixels | 75% (66%, 86%) | 22% (7%, 44%) | 24% (18%, 49%) | 46% (24%, 64%) | <0.001 | 3% (1%, 10%) |
| RPE Atrophy without overlying lesion | eyes | 20 (80%) | 14 (32%) | 0 (0%) | 4 (15%) | <0.001 | 20 (29%) |
| | % pixels | 25% (12%, 39%) | 1% (0%, 2%) | N/A | 2% (0%, 5%) | <0.001 | 1% (0%, 3%) |
| RPE Atrophy with overlying lesion | eyes | 25 (100%) | 42 (95%) | 4 (57%) | 23 (88%) | 0.005 | 58 (85%) |
| | % pixels | 52% (38%, 62%) | 22% (7%, 43%) | 24% (18%, 49%) | 46% (24%, 64%) | <0.001 | 3% (1%, 7%) |
| | | | | | | | |
| **Photoreceptor Loss** | eyes | 25 (100%) | 42 (95%) | 4 (57%) | 23 (88%) | 0.005 | 65 (96%) |
| | % pixels | 85% (66%, 92%) | 42% (22%, 61%) | 33% (22%, 67%) | 59% (33%, 78%) | <0.001 | 7% (3%, 19%) |
| **Outer Retinal Tubulation** | eyes | 9 (36%) | 21 (48%) | 1 (14%) | 11 (42%) | 0.40 | 15 (22%) |
| | % pixels | 1% (0%, 2%) | 1% (0%, 3%) | 4% (4%, 4%) | 1% (1%, 8%) | 0.49 | 0% (0%, 0%) |
| | | | | | | | |
| **Subretinal Lesion** | eyes | 20 (80%) | 42 (95%) | 7 (100%) | 26 (100%) | 0.04 | 65 (96%) |
| | % pixels | 31% (13%, 69%) | 42% (19%, 66%) | 85% (64%, 95%) | 92% (88%, 100%) | <0.001 | 3% (1%, 6%) |
| Sub-retinal hyper-reflective material (SHRM) | eyes | 14 (56%) | 28 (64%) | 4 (57%) | 22 (85%) | 0.11 | 37 (54%) |
| | % pixels | 27% (3%, 40%) | 8% (2%, 25%) | 16% (14%, 33%) | 71% (47%, 81%) | <0.001 | 0% (0%, 1%) |
| Pigment epithelial detachment (PED) | eyes | 19 (76%) | 42 (95%) | 7 (100%) | 26 (100%) | 0.01 | 64 (94%) |
| | % pixels | 18% (9%, 52%) | 32% (16%, 66%) | 72% (49%, 95%) | 80% (47%, 95%) | <0.001 | 3% (1%, 6%) |
| Indeterminate SHRM/PED | eyes | 13 (52%) | 23 (52%) | 3 (43%) | 9 (35%) | 0.49 | 27 (40%) |
| | % pixels | 3% (1%, 8%) | 2% (1%, 6%) | 9% (2%, 12%) | 4% (3%, 4%) | 0.66 | 0% (0%, 0%) |
| | | | | | | | |
| **Any Fluid** | eyes | 16 (64%) | 26 (59%) | 3 (43%) | 19 (73%) | 0.44 | 41 (60%) |
| | % pixels | 2% (0%, 16%) | 3% (0%, 23%) | 6% (2%, 25%) | 14% (1%, 49%) | 0.45 | 1% (0%, 2%) |
| Intra-retinal fluid (IRF) | eyes | 16 (64%) | 23 (52%) | 2 (29%) | 16 (62%) | 0.36 | 36 (53%) |
| | % pixels | 2% (0%, 14%) | 1% (0%, 3%) | 13% (1%, 25%) | 4% (1%, 18%) | 0.10 | 0% (0%, 1%) |
| Sub-retinal fluid (SRF) | eyes | 4 (16%) | 14 (32%) | 2 (29%) | 8 (31%) | 0.51 | 20 (29%) |
| | % pixels | 1% (0%, 1%) | 9% (0%, 30%) | 3% (1%, 6%) | 4% (1%, 43%) | 0.26 | 1% (0%, 6%) |

| OCT feature | | CP/FA component | | | | p | No CP/FA component |
|---|---|---|---|---|---|---|---|
| | | Geographic Atrophy (GA) n=25 | Non-Geographic Atrophy (NGA) n=44 | Non-Fibrotic Scar (NFS) n=7 | Fibrotic Scar (FS) n=26 | | Macular area outside total CNV lesion, n=68 |
| | eyes containing any pixels of OCT feature | n (%) | n (%) | n (%) | n (%) | | n (%) |
| | percent of pixels with OCT features within the CP/FA component* | Median (25%, 75%) | Median (25%, 75%) | Median (25%, 75%) | Median (25%, 75%) | | Median (25%, 75%) |
| Sub-RPE fluid | eyes | 3 (12%) | 8 (18%) | 0 (0%) | 4 (15%) | 0.82 | 6 (9%) |
| | % pixels | 0% (0%, 3%) | 1% (0%, 10%) | N/A | 26% (6%, 53%) | 0.26 | 0% (0%, 0%) |
| **Absent the above OCT features** | eyes | 23 (92%) | 43 (98%) | 4 (57%) | 18 (69%) | <0.001 | 68 (100%) |
| | % pixels | 6% (3%, 12%) | 27% (12%, 54%) | 20% (10%, 27%) | 3% (1%, 9%) | <0.001 | 87% (74%, 94%) |

* Percentage of pixels in the CP/FA component is only from those eyes that contained any of the respective OCT feature: e.g. In 42 eyes with NGA a median of 22% of pixels contained the OCT feature of RPE Atrophy

RPE = retinal pigment epithelium; Subretinal Lesion includes: SHRM, PED and Indeterminate SHRM/PED;

One eye may have multiple CP/FA components.

**Table 2:**

Cross tabulations between the different optical coherence tomography (OCT) features per overlay pixel at year 2 in CATT.

| OCT feature | RPE Atrophy with choroidal hypertransmission | RPE Atrophy without overlying lesion | RPE Atrophy with overlying lesion | Photoreceptor Loss | Outer Retinal Tubulation | Subretinal Lesion | Sub-retinal hyper-reflective material (SHRM) | Pigment epithelial detachment (PED) | Indeterminate SHRM/PED | Any Fluid | Intra-retinal fluid (IRF) | Sub-retinal fluid (SRF) | Sub-RPE fluid |
|---|---|---|---|---|---|---|---|---|---|---|---|---|---|
| | **6,981,000 pixels** | **1,077,989 pixels** | **5,909,746 pixels** | **9,257,940 pixels** | **216,104 pixels** | **9,010,256 pixels** | **3,314,457 pixels** | **7,303,084 pixels** | **471,373 pixels** | **2,200,032 pixels** | **680,183 pixels** | **1,262,014 pixels** | **401,330 pixels** |
| **RPE Atrophy** with choroidal hypertransmission | 100.00% | 100.00% | 100.00% | 56.90% | 59.40% | 34.20% | 51.80% | 27.40% | 58.00% | 19.50% | 32.60% | 16.00% | 3.70% |
| RPE Atrophy without overlying lesion | 15.40% | 100.00% | 0.10% | 10.90% | 2.50% | 0.50% | 1.10% | 0.10% | 0.20% | 0.10% | 0.40% | < 0.01% | 0% |
| RPE Atrophy with overlying lesion | 84.70% | 0.60% | 100.00% | 46.00% | 56.90% | 33.80% | 50.70% | 27.30% | 57.70% | 19.40% | 32.20% | 16.00% | 3.70% |
| **Photoreceptor Loss** | 75.50% | 93.90% | 72.10% | 100.00% | 44.40% | 42.50% | 54.40% | 37.50% | 54.40% | 18.20% | 37.20% | 10.10% | 7.90% |
| **Outer Retinal Tubulation** | 1.80% | 0.50% | 2.10% | 1.00% | 100.00% | 1.80% | 3.60% | 1.90% | 1.50% | 0.20% | 0.70% | 0% | < 0.01% |
| **Subretinal Lesion** | 44.10% | 3.80% | 51.50% | 41.40% | 76.80% | 100.00% | 100.00% | 100.00% | 100.00% | 68.60% | 79.20% | 56.00% | 99.50% |
| Sub-retinal hyper-reflective material (SHRM) | 24.60% | 3.30% | 28.40% | 19.50% | 54.60% | 36.80% | 100.00% | 25.40% | 5.40% | 24.10% | 40.40% | 19.00% | 10.60% |
| Pigment epithelial detachment (PED) | 28.70% | 0.60% | 33.80% | 29.60% | 62.90% | 81.10% | 55.90% | 100.00% | 47.30% | 63.40% | 72.20% | 50.90% | 98.80% |
| Indeterminate SHRM/PED | 3.90% | 0.10% | 4.60% | 2.80% | 3.20% | 5.20% | 0.80% | 3.00% | 100.00% | 3.70% | 9.90% | 0.70% | 1.90% |
| **Any Fluid** | 6.10% | 0.30% | 7.20% | 4.30% | 2.10% | 16.80% | 16.00% | 19.10% | 17.10% | 100.00% | 100.00% | 100.00% | 100.00% |
| Intra-retinal fluid (IRF) | 3.20% | 0.30% | 3.70% | 2.70% | 2.10% | 6.00% | 8.30% | 6.70% | 14.20% | 30.90% | 100.00% | 2.30% | 5.00% |
| Sub-retinal fluid (SRF) | 2.90% | < 0.01% | 3.40% | 1.40% | 0% | 7.80% | 7.20% | 8.80% | 1.80% | 57.40% | 4.30% | 100.00% | 23.80% |
| Sub-RPE fluid | 0.20% | 0% | 0.30% | 0.30% | < 0.01% | 4.40% | 1.30% | 5.40% | 1.60% | 18.20% | 3.00% | 7.60% | 100.00% |

The column is all pixels with that column's feature, and the row is the percentage of that row's feature that appear in the column feature.

RPE = retinal pigment epithelium; Subretinal Lesion includes: SHRM, PED and indeterminate SHRM/PED;